Crucial Role of the Residue R280 at the F′–G′ Loop of the Human Granulocyte/Macrophage Colony-stimulating Factor Receptor α Chain for Ligand Recognition

By D. Rajotte,*¶ C. Cadieux,*¶ A. Haman,* B.C. Wilkes,‡§ S.C. Clark,** T. Hercus,‡‡ J.A. Woodcock,‡‡ A. Lopez,‡‡ and T. Hoang*§‖¶

*From the *Clinical Research Institute of Montréal, Laboratory of Hemopoiesis and Leukemia, and ‡Laboratory of Biological Chemistry, Montréal, Quebec H2W 1R7, Canada; §Department of Pharmacology, ‖Department of Biochemistry, and ¶Department of Molecular Biology, University of Montréal, Montréal, Quebec H3C 3J7, Canada; **The Genetics Institute, Cambridge, Massachusetts 02140; and ‡‡Hanson Cancer Center, Adelaide 5000, Australia*

Summary

The receptor for granulocyte/macrophage colony-stimulating factor (GM-CSF) is composed of two chains, α and βc. Both chains belong to the superfamily of cytokine receptors characterized by a common structural feature, i.e., the presence of at least two fibronectin-like folds in the extracellular domain, which was first identified in the growth hormone receptor. The GM-CSF receptor (GMR)-α chain confers low affinity binding only (5–10 nM), whereas the other chain, βc, does not bind GM-CSF by itself but confers high affinity binding when associated with GMR-α (25–100 pM). The present study was designed to define the assembly of the GMR complex at the molecular level through site-directed mutagenesis guided by homology modeling with the growth hormone receptor complex. In our three-dimensional model, R280 of GMR-α, located in the F′–G′ loop and close to the WSSWS motif, is in the vicinity of the ligand Asp112, suggesting the possibility of electrostatic interaction between these two residues. Through site directed mutagenesis, we provide several lines of evidence indicating the importance of electrostatic interaction in ligand–receptor recognition. First, mutagenesis of GMR-αR280 strikingly ablated ligand binding in the absence of β common (βc); ligand binding was restored in the presence of βc with, nonetheless, a significant shift from high (26 pM) toward low affinity (from 2 to 13 nM). The rank order of the dissociation constant for the different GMR-αR280 mutations where Lys > Gln > Met > Asp, suggesting the importance of the charge at this position. Second, a mutant GM-CSF with charge reversal mutation at position Asp112 exhibited a 1,000-fold decrease in affinity in receptor binding, whereas charge ablation or conservative mutations were the least affected (10–20-fold). Third, removal of the charge at position R280 of GMR-α introduced a 10-fold decrease in the association rate constant and only a 2-fold change in the dissociation rate constant, suggesting that R280 is implicated in ligand recognition, possibly through interaction with Asp112 of GM-CSF. For all R280 mutants, the half-efficient concentrations of GM-CSF required for membrane (receptor binding) to nuclear events (c-fos promoter activation) and cell proliferation (thymidine incorporation) were in the same range, indicating that the threshold for biologic activity is governed mainly by the affinity of ligand–receptor interaction. Furthermore, mutation of other residues in the immediate vicinity of R280 was less drastic. Sequence alignment and modeling of interleukin (IL)-3R and IL-5R identified an arginine residue at the tip of a β turn in a highly divergent context at the F′–G′ loop, close to a conserved structural element, the WSXWS motif, suggesting the possibility of a ligand association mechanism similar to the one described herein for GMR.

C. Cadieux and D. Rajotte contributed equally to this work.

 J. Exp. Med. © The Rockefeller University Press • 0022-1007/97/06/1939/12 $2.00
Volume 185, Number 11, June 2, 1997 1939–1950

Human GM-CSF is a cytokine that promotes the proliferation, survival, and functional activation of cells in the granulocytic and monocytic lineage (1–4). Gene cloning indicates that the receptor for GM-CSF is composed of two chains, α (5) and β (6). The human GM-CSF receptor (GMR)-α subunit is 378 amino acid (aa)[1] in length (5), most of which constitutes the extracellular domain. GMR-α confers low affinity binding and has been shown to be species specific for its ligand (5, 7), whereas β, which is required for signal transduction, comprises 881 aa with a 432 aa cytoplasmic tail (6). Both α and β cytoplasmic domains lack intrinsic enzymatic activities. Interestingly, the β chain, referred to as β common or βc, is shared with the receptors for IL-3 and -5, two cytokines that exhibit significant overlap in biological activity with GM-CSF (for review see reference 8). Our previous data suggest that the transition from low affinity to high affinity binding results from the association of βc to the GM-CSF–GMR-α complex, resulting in a more stable ternary complex (9). Data from many groups also suggest that only the high-affinity receptor mediates the biologic response of the cells to GM-CSF (3, 5, 7). Expression of the two chains of the GM-CSF receptor in NIH 3T3 cells results in GM-CSF–induced signal transduction (10), morphological transformation (11, 12), and cell proliferation (13).

Both chains of the GM-CSF receptor are members of the superfamily of cytokine receptors, characterized by conserved structural features in the extracellular domain, i.e., four conserved cysteine residues, and a typical WSXWS motif in the juxtamembrane region. According to the model predicted by Bazan (14), cytokine receptors are made up of two domains, each containing seven antiparallel β strands similar to the fibronectin fold. These strands are coded A–G for the NH_2-terminal domain and A′–G′ for the COOH-terminal domain. Together, these two domains form a common cytokine receptor motif (CRM). This predicted structure was confirmed through crystallization of the growth hormone (GH)–GHR complex (15) and of the tenth type III segment of human fibronectin (16). The tenth segment of fibronectin has, in fact, been shown to bind integrin through the RGD site located at the F–G loop. Furthermore, scanning mutagenesis of IL-6R-α also identified several residues in the same region, E278/F279, and surrounding residues (A275, G282/E283) as essential for IL-6 binding (17). These data indicate a clustering of residues that are important in ligand–receptor recognition at the F′–G′ loop of the CRM.

GMR-α plays a critical role in receptor complex formation because it confers the specificity of association with the ligand and it is involved in signal transduction as shown by our team (12) and others (18). Therefore the aim of this work was to identify the molecular determinants of the complex formation on GMR-α, through site directed mutagenesis guided by homology modeling based on the GH–GHR complex. Functionally important residues have to be in the vicinity of residues on the ligand that are crucial for receptor binding and to be located in a divergent context compared to IL-3R-α and -5R-α. We have thus identified the critical role of R280 located at the F′–G′ loop of GMR-α in ligand binding.

Materials and Methods

Homology Modeling of the GM-CSF Hormone Receptor Complex. All calculations were performed using the software package SYBYL (Tripos Assoc., St. Louis, MO) on a SiliconGraphics Indigo²-Extreme workstation. The Kollman united atom force field was used for energy calculations, and a dielectric constant of 10 was used to approximate a protein receptor environment. The x-ray crystal structure of human growth hormone (hGH) bound to its receptor (15) was obtained from the Brookhaven protein database. Before manipulations, the entire complex was subjected to 1,000 steps of conjugate gradient minimization. GMR-α has one CRM as GHR, whereas βc has a duplicated extracellular domain with two such CRM. Using the sequence alignment of Goodall et al. (19) the extracellular domain of molecule 1 (GHRI) and GHRII chains of the GH–GHR_2 complex were transformed one amino acid at a time into the GM-CSF receptor α chain and the membrane proximal CRM motif of βc, respectively. The backbone dihedryl angles were held fixed to preserve the receptor's secondary structure, whereas the amino acid side chains were positioned using the scan subroutine in SYBYL. This routine rotates each side chain dihedryl angle until a sterically acceptable conformation was obtained. The x-ray crystal structure of GM-CSF has been reported (20). The hGH ligand was excised from the hormone receptor complex and the GM-CSF ligand was positioned into the receptor visually in approximately the same orientation and position as was hGH. When the new ligand–receptor complex displayed reasonable steric complementarity, the entire complex was minimized as above, allowing all atoms to relax. A molecular dynamics simulation of 20 ps was performed to determine the stability of the GM-CSF receptor complex, and it was determined that the complex retained its secondary structure. Point mutations of the new GM-CSF receptor and hormone were performed using the same methodology, and the stability of each new complex was determined using energy calculations as well as short (5–10 ps) molecular dynamics simulations.

The same approach was used to construct the model of IL-3, -5, and Epo hormone receptor complex. Since the crystal structures of IL-3 and Epo are not available, we used the GM-CSF and GH coordinates as templates for the hormone in the IL-3 and Epo receptor complex models, respectively, for the following reasons. On one hand, structure prediction for IL-3 (21) and nuclear magnetic resonance data of a human IL-3 variant (22) show that the IL-3 structure is folded into the same up-up-down-down arrangement of the four helices bundle observed for the GM-CSF structure. On the other hand, the α helices of erythropoietin are longer and Epo is classified as a long chain helical-bundle subclass, to which belongs growth hormone (23).

Site-directed Mutagenesis of Human GM-CSF and of GMR-α. The human GM-CSF cDNA was mutated at the indicated positions (Table 1), expressed in *Escherichia coli* and purified as described (24). The GMR-α cDNA was cloned in the expression vector pME18S (10). The cDNA for βc (KH97) was cloned in

[1]*Abbreviations used in this paper:* βc, β common; aa, amino acid; CHO, Chinese hamster ovary; CRM, cytokine receptor motif; GH, growth hormone; GMR, GM-CSF receptor; hGH, human growth hormone; NIH, National Institutes of Health.

Table 1. *Binding of Mutant GM-CSF to Wild-type GMR-α*

GM-CSF position	Mutation	Kd
		nM
Wild type	–	1.7
E 108	A	3.8
	Q	8.1
	K	3.0
N 109	D	2.8
	A	15.0
	K	7.9
K 111	A	1.4
	Q	2.7
	E	2.1
D 112	N	19
	A	31
	R	335
	K	1,400

CHO cells expressing the GMR-α chain were generated as described in Materials and Methods. Mutations in GM-CSF were introduced at the indicated position by site directed mutagenesis and expressed in *E. coli*. Kds of the various purified GM-CSF mutants were determined by competition analysis on GMR-α–transfected CHO cells.

the same vector, but without the neomycin selectable gene. Both were provided by Dr. Toshio Kitamura (DNAX, Palo Alto, CA). GMR-α cDNA bearing point mutations at position R280 were generated by PCR site-directed mutagenesis. The forward oligos used to generate the various point mutations were tcagagctgcagacgtcgaaatctt (GMR-αR280E), tcagagctgcagacgtcaagatctt (GMR-αR280K), tcagagctgcagacgtcatgatctt (GMR-αR280M), and tcagagctgcagacgtccagatctt (GMR-αR280Q). In all reactions, the reverse oligo used was gctttatttgtgaaatttgtgatg. The pME18 vector containing the full GMR-α cDNA was used as a template for PCR reactions and the annealing temperature was 58°C. Purified PCR fragments of mutated GMR-α were digested by PstI and inserted into the same site of the complete GMR-α cDNA cloned into the pGEM7 vector (Promega Corp., Madison, WI). Excised EcoRI fragments of pGEM7 vector containing a mutant version of GMR-α were inserted into the same site of the pME18S expression vector containing the full GMR-α cDNA. Resulting clones were sequenced to confirm presence of the point mutation and that no other mutations were present in the PCR amplified region.

Double mutations at two positions, Asp278Val279 (D278V279) and Ile281Leu282 (I281L282), as well as single mutations of Asp278 (D278) were generated through a similar approach with the following primers aagatcagagctgcagccgcccgcatct (GMR-αD278-AV279A), tgaagatcagagctgcacagcagcgcatct (GMR-αD278QV27-9Q), tgaagatcagagctgcagccgtccgcatct (GMR-αD278A), tgaagatcagagctgcaaacgtccgcatct (GMR-αD278N), atcagagctgcagacgtccgcgccgccaattgg (GMR-αI281AL282A), and atcagagctgcagacgtccgccagcagaattgg (GMR-αI281QL282Q).

Transient Expression of GMR-α and βc at the surface of NIH 3T3. The GMR-α and βc cDNA were co-transfected by the calcium phosphate method (12, 13) in exponentially growing NIH 3T3 cells at a 1:1 ratio. In brief, 1 d before transfection, 200,000 cells were seeded in 60-mm tissue culture dishes. On the day of transfection, 400 μl of DNA-$Ca_3(PO_4)_2$ precipitate containing 12 μg of DNA was added to the culture and incubated for 16 h. Cells were then washed with PBS and split into replicate 24-well plates at a concentration of 75,000 cells/well. Each day after plating, the cells were used for either binding, cross-linking, or proliferation assays. Kinetics studies indicate the GM-CSF binding and GM-CSF–dependent cell proliferation was optimal on day 2 after transfection (data not shown). This time point was selected for all subsequent experiments.

Chinese hamster ovary (CHO) cell lines stably expressing the low affinity GMR-α were isolated as described previously (24).

Iodinated GM-CSF Binding Assays. Purified recombinant GM-CSF was iodinated with the Bolton–Hunter reagent (DuPont–New England Nuclear, Wilmington, DE). The specific activity of the radioligand was determined by radioimmunoassay (7) and confirmed independently by ELISA (25). NIH 3T3 cells were co-transfected with wild-type or mutant GMR-α and βc chain by the Ca-PO_4 method as described. After an overnight incubation, transfected cells were seeded to half confluency in 24-well culture dishes. 2 d after transfection, ligand-binding assay was performed at 4°C for 3 h in IMDM (without bicarbonate) supplemented with 1% BSA. Nonspecific binding was determined in the presence of 100-fold excess unlabeled GM-CSF. After binding, cells were washed twice with ice-cold PBS and collected by the addition of 200 μl of trypsin. Concentrations of radioligands used for all saturation curves were in the range of 20 pM–20 nM as indicated. Complete competition curves were performed with 500 pM of wild-type radioligand and varying concentrations of wild-type or mutant GM-CSF that were in the range of 0–40 nM. Binding constants were estimated through computer modeling with the program ALLFIT, based on a nonlinear curve fitting routine as described previously (7, 9, 26).

Kinetics of GM-CSF Binding. The association rate constants (K_{on}) were estimated by analysis of the kinetics of association at three different concentrations of radioligand for a time range of 5–120 min using the following equations. First, the kinetics of association for increasing concentrations of radioligand were subjected to linear transformation using the equation $\ln (B_e/[B_e - B_t]) = K_{ob} \times t$, where B_e is the observed binding at equilibrium and B_t the binding observed at a given time *t*. Linear regression of the slopes of these lines (K_{ob}) as a function of ligand concentrations provided an estimate of the association rate constant K_{on}. For dissociation experiments, ^{125}I–GM-CSF binding was performed at equilibrium at a concentration of 2 nM of radioligand. Cells were then incubated with a 100-fold excess of cold GM-CSF in IMDM 1% BSA for time periods ranging from 5 to 110 min. Supernatants were removed before counting of bound GM-CSF. The dissociation rate constant (K_{off}) was estimated using the following equation: $\ln (B_t/B_o) = -K_{off} \times t$ where B_o is the specific binding at equilibrium before dissociation, and B_t is the specific binding remaining after a period of *t* minutes.

Immunodetection of GMR-α, Cell Proliferation, and c-fos Promoter Assay. Surface expression of wild-type and mutant GMR-α were quantitated by whole cell immunoperoxidase assay using the monoclonal mouse anti–human GMR-α (Upstate Biotechnology Inc., Lake Placid, NY) as described previously (12). Cell proliferation was assessed by tritiated thymidine (DuPont–New England Nuclear) incorporation at a final concentration of 3 μCi/ml in serum-free medium (13) 48 h after transfection. The wild-type c-fos promoter luciferase reporter construct (3 μg) (17) was co-transfected with the various GMR-α (3 μg) and wild-type βc (3

μg) in NIH 3T3 by the calcium-phosphate method. Transiently transfected cells were then incubated for 24 h in serum-free medium in the presence or absence of GM-CSF, lysed, and luciferase activity was determined in nuclear extract as described (13) after adjustment for growth hormone activity driven by the Rous sarcoma virus LTR (2 μg), which was co-transfected as an internal control.

Results

Modeling GM–GMR Interaction Based on the Crystal Structure of the GH–GHR Complex. The initial event in GH binding to its receptor is the association of site 1 on GH with GHRI to form a 1:1 complex (binding affinity, dissociation constant [Kd] = 0.3 nM), followed by the association of site 2 with GHR molecule 2 (GHRII) to form a ternary complex GH–GHR_2 (27, 28). The first binding step involving GHRI results in the burial of a 1,230-Å surface, whereas only 900 Å is buried on binding of GHRII, consistent with a higher affinity of interaction of GHRI with site 1. The modeling for GMR-α is therefore based on GHRI interaction with site 1 and for βc on GHRII interaction with site 2. Our model identifies a contact surface between βc and the ligand that includes H367 on βc (29, 30) and residue E21 (31) on the ligand as previously documented (Fig. 1). Finally, domains of the ligand that appear to be involved in intermolecular contacts correspond to those identified previously through the use of human mouse chimeras (32), and of truncated GM-CSF (33) i.e., helix A, the AB loop, and helix D.

Importance of the Negative Charge at Position 112 of GM-CSF Defined by Site-directed Mutagenesis. Modeling identified several hydrophilic and charged surface residues of helix D of GM-CSF as potential contact points with GMR-α: E108, N109, K111, and D112. Sequence analysis indicates that these are aligned with residues that are shown to be at the interface of growth hormone with GHRI (28). Mutations at two of these residues on GM-CSF, E108 and D112, were previously shown to decrease ligand–receptor binding (24). We therefore generated further mutations at all four positions identified by modeling. Quantitative analysis of GM-CSF binding to CHO cells stably expressing GMR-α alone was determined through complete competition curves for each mutant using wild-type radioligand as a marker (Table 1). Our data indicate that charge removal (Lys→Ala; Lys→Gln) or charge reversal (Lys→Glu) at residue K111 did not significantly affect GM–GMR-α recognition. Similarly, mutations at positions E108 and N109 resulted only in a 2–9-fold shift in affinity as compared to wild-type ligand. Finally, the most drastic effect was seen with the D112 mutants; there was a 12–800-fold shift in Kd depending on the mutation, and the rank order was D112N < D112A < D112K. Thus, the least affected was the Asp to Asn mutation, which represents a shift in isoelectric point from 3 to 5.4. In addition, the Kd of Asp to Ala substitution was only slightly higher than that of the Asn mutant. In contrast, it is revealing that the charge reversal mutants (Asp→Lys and Asp→Arg) resulted in a drastic shift in Kd to the right. This rank order indicates that

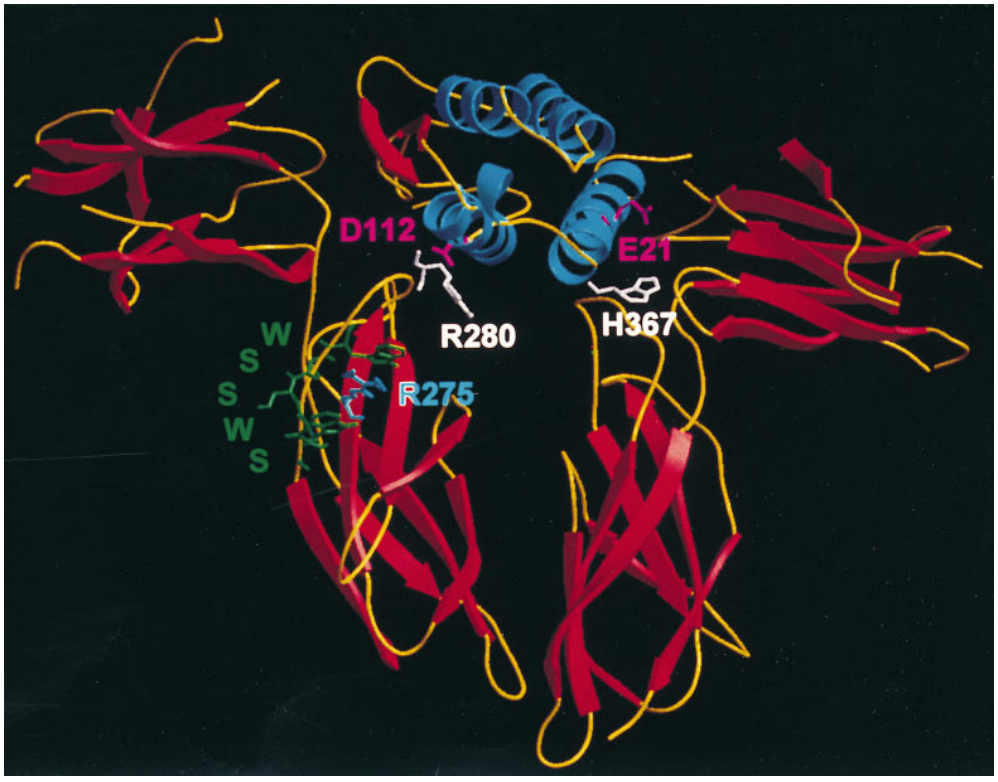

Figure 1. Homology modeling of the GM-CSF receptor complex with its ligand on the basis the crystal structure of the growth hormone complex. The extracellular domains of GMR-α (*left*) and membrane proximal CRM of βc (*right*) are shown complexed with GM-CSF, each receptor chain being organized in two fibronectin-like domains with seven β strands. This representation of the GM–GMR complex is based on the structure of the GH–GHR_2 complex and was generated as described in the Materials and Methods. α helices are shown in blue and β strands in red. Two basic surface residues (*white*) that are potentially involved in electrostatic interaction with surface residues (*magenta*) on the ligand are highlighted. The location of the conserved WSXWS motif is shown in green. R275 located on the F′ strand, potentially involved in π-cation interaction with the two Trp residues of the WSSWS box (similarly observed in the crystal structure of EpoR complexed with a peptide ligand, 40), is shown in blue.

the interaction between D112 and the receptor is mainly electrostatic.

Proximity of R280 of GMR-α and D112 of the Ligand. Because of the importance of the charge at position 112 of the ligand, the residues surrounding D112 were further evaluated in the ligand–receptor binding pocket of the three-dimensional GM–GMR model shown in Fig. 1. The acidic residue D112 is oriented towards GMR-α and is positioned at a distance of 3–4.7 Å from the basic residue R280. The estimated distance remains within the possibility of intermolecular interaction at this position. For example, E21 on GM-CSF is located within 4.19 Å of H367 on βc. We therefore proceeded to site-directed mutagenesis of R280 of GMR-α.

Loss of GM-CSF Binding to the GMR-αR280 Mutants. Several mutations were introduced at this position on the basis of charge conservation (R280K), charge removal (R280Q), and hydrophilic to hydrophobic conversion (K280M) or charge reversal (R280E). NIH 3T3 cells were transiently transfected with these various GMR-α mutants alone and submitted to GM-CSF binding assays. All of the mutants showed a complete loss of specific binding compared to the wild-type GMR-α chain at 2 nM of iodinated GM-CSF (Fig. 2 *A*), a concentration shown to be in the range of the Kd of the low affinity GM-CSF binding site. Even at high concentrations of GM-CSF (i.e., 8–20 nM) we did not detect any specific binding for three mutants tested, R280K, R280M, and R280E (data not shown). All GMR-αR280 mutants were detected by the anti–GMR-α antibody in an immunoperoxidase assay (Fig. 2 *B*). This indicates that the mutations did not induce important structural changes or modification of the expression level of GMR-α. Furthermore, mutation of another surface Arg into Gln, R258Q, did not affect ligand binding in the absence (data not shown) or in the presence of βc (see Table 3). These data underscore the crucial role of R280 in GM-CSF binding by GMR-α.

Physical Interaction of Mutated GMR-α with βc Restores Ligand Binding with Intermediate to Low Affinity. GM-CSF binding assays were performed with mutated GMR-α and βc. Surprisingly, specific binding was detected in all cases, but was drastically reduced as compared to the wild-type receptor (Fig. 3 and Table 2). Cotransfection of wild-type GMR-α and βc results in both high and low affinity GM-CSF binding (6). In contrast, all GMR-α R280 mutants exhibit a single GM-CSF binding site of intermediate to low affinity with Kds in the following order: R280K < R280Q < R280M < R280E. The extensive loss of binding of GMR-α R280E in presence of βc indicates a charge effect at this position. As βc alone does not bind the ligand (data not shown), one can conclude that a mutated GMR-α can associate with wild-type βc to form a lower affinity complex.

Association between GMR-α and βc may create additional contact points between GMR-α and the ligand itself, in addition to R280. To address this question, we cotransfected the mutant αR280M with either wild-type βc or βH367A that can no longer form a high affinity GM-CSF complex. In contrast to wild-type βc, cells expressing

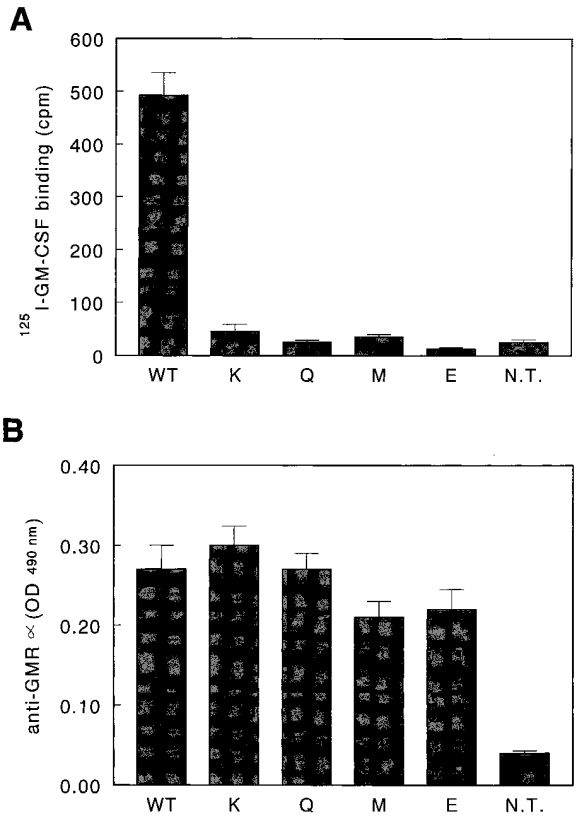

Figure 2. Binding of wild-type GM-CSF to mutant GMR-α. NIH 3T3 cells were transiently transfected with wild-type or mutant forms of the GMR-α chain (R280K, R280Q, R280M, R280E) as described in Materials and Methods. (*A*) Triplicate cultures of transfected or nontransfected (*N.T.*) cells were incubated with 2 nM of ^{125}I–GM-CSF. Nonspecific binding was determined by incubation with 2 nM ^{125}I–GM-CSF and 100-fold excess of nonradiolabeled ligand. The residual amount of ^{125}I–GM-CSF binding (<50 cpm) was reproducibly observed in nontransfected NIH 3T3 cells due to incomplete competition of nonspecific binding. (*B*) Triplicate cultures of transfected or nontransfected (*N.T.*) cells were tested for GMR-α surface expression using an immunoperoxidase assay as described in Materials and Methods. There is a low level of endogenous peroxidase activity (<0.04) in untransfected cells because the surface expression of GMR-α was determined on intact cells.

αR280M and βH367A were unable to bind GM-CSF (Fig. 3). Hence, preassociation with βc is unlikely to create additional contact points between GMR-α and the ligand apart from those that are affected by the mutations.

Comparative Kinetics of Binding of R280M Mutant and Wild-type GMR-α. Previous observations (5, 34) suggest that the difference in Kd between low (GMR-α alone) and high (GMR-α–βc) affinity GM-CSF binding sites is mainly due to differences in the dissociation rate constants, whereas the association rate constants are in the same range. We therefore compared the binding kinetics of mutant GMR-αR280M with that of wild-type GMR-α. The association rate constant (on rate) was 10-fold lower for the mutant receptor, as compared to the wild-type receptor (Fig. 4 and Table 3). In contrast, there was only a twofold difference in the dissociation rate constants (off rate). These results suggest that the 20–30-fold decrease in binding affinity ob-

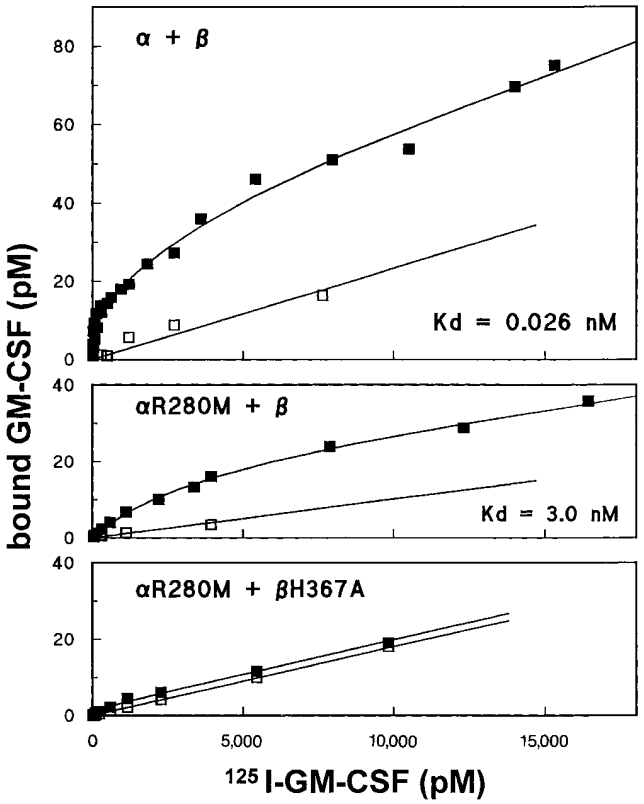

Figure 3. Binding of wild-type GM-CSF to mutant GMR-α co-transfected with wild-type or mutant βc. NIH 3T3 cells were transiently co-transfected with either wild-type or mutant GMR-αR280M and wild-type βc or βcH367A. ^{125}I–GM-CSF saturation assays were performed as described in Materials and Methods and Table 2. Data are typical of at least two independent experiments. The curves passing through the data were calculated with the program ALLFIT (9, 26). For wild-type α and βc, data were better described by a two-binding site model (high and low affinity), whereas the data observed with αR280M mutant and wild-type βc were better described by a one binding site model (low affinity only). There was no binding when αR280M were coexpressed with βH367A. Kd values obtained for all GMR-α mutants are shown in Table 2.

Table 2. *Binding of Wild-type GM-CSF by Mutated GMR-α in Association with βc*

α + wt β	Kd	EC_{50}
	nM	*nM*
wt	0.03	0.08
R280K	0.9	1.8
R280Q	1.7	3.0
R280M	2.8	2.5
R280E	13	15.1

NIH 3T3 cells were transiently transfected with the indicated GMR-α mutants and wild-type (*wt*) βc. Dissociation constants determined by saturation analysis and competition analysis with ^{125}I–GM-CSF were similar. Data shown were determined by saturation analysis, using radioligand concentrations that were in the range of 5 pM–30 nM. Nonspecific binding was determined through the addition of a 200-fold excess of cold GM-CSF. With wild-type GMR-α and βc, the data were better described by a two-site model, a high-affinity binding site as shown in the first row, and a low-affinity binding site of 2–20 nM, which were also the values observed with GMR-α alone. In contrast, in the presence of mutant GMR-α and wild-type βc, the data were better described by a one binding site equation. Half-efficient concentration (EC_{50}) for GM-CSF were estimated by analysis of the proliferation curves shown in Fig. 5 with the program ALLFIT.

served for the GMR-αR280M mutant compared to wild-type GMR is mainly due to a decrease in the association rate constant. In comparison, mutation of another Arg residue, R258Q, did not significantly affect the kinetic constants (Table 3). Thus, the charge at position R280 of GMR-α is essential for ligand recognition and association, which is different from the role assigned to βc, i.e., stabilization of the complex through a decrease in the dissociation rate of the ligand.

The contribution of other residues in the F′–G′ loop surrounding R280 was next defined (Table 3). Neither Ile281 nor Leu282 were affected by alanine substitution, whereas a change to a hydrophilic residue (Gln) slightly affected the on rate. We also found that the negative charge at position 278 was almost as important as the positive charge at position 280 since mutation from Asp to Asn, which removed the charge, reduced the on rate by 10-fold. The immunoreactivity of D278 mutants with the monoclonal anti-GMR-α was reproducibly two- to three-fold higher than that of wild-type GMR-α suggesting that the consequence of the mutation was not confined to the Asp residue, but may also have affected a local structure. Indeed the immunoreactivity of all other mutations was unaffected, and furthermore, their surface expression was not affected in binding assays (as assessed by the maximum binding capacity, data not shown). Thus charge removal at position 278 may result in a better unfolding of the epitope recognized by anti–GMR-α. The three-dimensional model indicates that Asp278 is oriented towards Lys191 located in the linker region between the two fibronectin folds of GMR-α, suggesting a role in stabilization of GMR-α structure through electrostatic interaction.

Correlation Between Ligand Binding and the Biologically Active Threshold for the Mutant GMR-αR280–βc Complex. A proliferation assay was performed on transiently transfected NIH 3T3 cells incubated for 40 h in serum-free medium in the absence or in the presence of GM-CSF. In cells expressing the wild-type receptor, GM-CSF induces a dose-dependent increase in thymidine uptake with a plateau stimulation at 1 nM (Fig. 5). When the wild-type GMR-α chain was substituted by R280K, R280M, or R280Q mutants, higher concentrations of GM-CSF were needed to obtain a response, but a maximal induction of 2.5-fold could still be observed. For the R280E mutant, only a weak proliferative response could be detected at 10 nM of GM-CSF. The half-efficient concentrations for stimulation of cell proliferation were in the same range as the Kd of the receptor complex (Table 2). Similarly, stimulation of c-fos promoter activity by GM-CSF followed the shift in Kd as above (Fig. 5). The mutated receptor is, therefore,

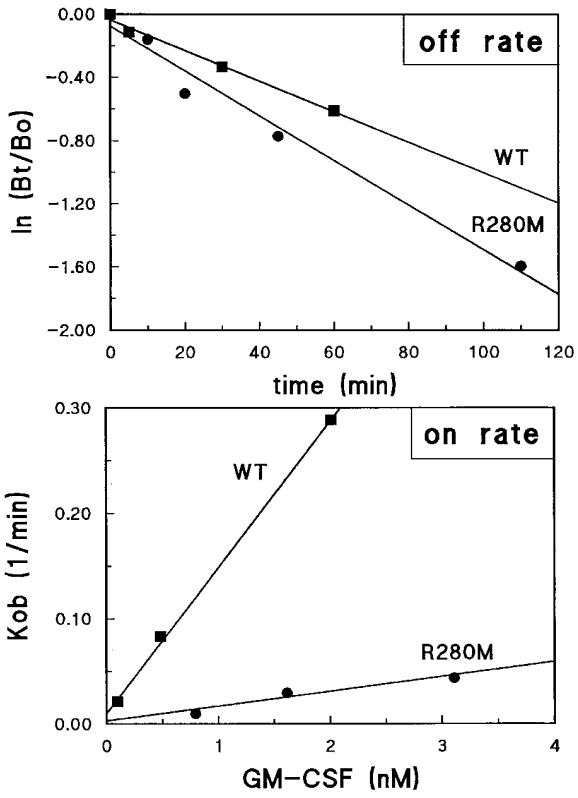

Figure 4. Comparison of the kinetics for binding of wild-type GM-CSF to wild-type GMR-α or R280M mutant co-transfected with wild-type βc. Linear transformation of the dissociation curves are shown in upper panel and of the association curves in lower panel. The slopes of theses lines provide an estimate of the dissociation rate constants (K_{off}) and the association rate constants (K_{on}), respectively, shown in Table 3. B_0, GM-CSF–specific binding at time 0; B_t, GM-CSF specifically bound at time t; K_{ob}, the slope of ln ($B_{eq}/[B_{eq} - B_t]$) as a linear function of t; B_{eq}, GM-CSF–specific binding at equilibrium; *WT*, wild type.

still competent for initiating a biological response at concentrations of GM-CSF that are in the range of the Kd as shown previously (3, 7). These data underscore the importance of GMR-α and of appropriate receptor assembly in signaling. Furthermore, the threshold for biologic activity is most likely governed by the affinity of ligand–receptor interaction.

Discussion

In the present study, we provide evidence for an essential contribution of R280 in establishing a salt bridge with GM-CSF when binding was performed in the absence of βc. Similarly, Asp112 on the ligand appears to play a crucial role in receptor binding. The proximity of R280 on GMR-α with Asp112 on the ligand strongly supports the possibility of electrostatic interaction between these two residues. In the presence of wild-type βc, our data indicate that R280 contributes to high affinity GM-CSF binding since mutations at this position result in a significant shift towards low affinity binding. Together, our observations indicate the crucial role of a single charged residue at the F′–G′ loop of GMR-α in GM-CSF binding R280 that interacts with an acidic residue on the ligand, most likely Asp112.

Importance of the Charge at Positions R280 of GMR-α and Asp112 of GM-CSF. Mutagenesis of a single residue can potentially introduce structural perturbations that alter protein–protein interaction at positions not directly involved in establishing contact points. In the case of GMR-α, given the large size of Arg and its location at the tip of the loop, we chose to substitute Arg with residues of larger chain size than Ala, which is a common choice for substitution, for the purpose of steric complementarity. In addition, all mutant proteins reacted equally with a neutralizing monoclonal antibody directed against wild-type GMR-α. This suggests that mutations at position R280 of GMR-α are likely localized to this residue without affecting the overall structure of the protein.

The importance of the charge at positions R280 of GMR-α and Asp112 of the ligand was inferred from the rank order of a series of mutations that introduce a reduction in charge, a change in hydrophilic to hydrophobic residue, or simply charge reversal. Among GMR-α mutants evaluated in the context of wild-type βc, R280M and R280Q behaved similarly because of a decrease in charge at this position, whereas the conservative mutation R280K was the least affected, and the charge reversal R280E was drastically shifted in affinity. Similarly, mutations at Asp112 of GM-CSF displayed the expected rank order with the charge reversal being the most drastically affected, whereas homologous mutations at positions not crucial for receptor binding, i.e., N109 or K111, were almost silent. Nonetheless, we were not able to observe a complementation between GM-CSF–D112K and GMR-α–R280E mutants, possibly because mutations on the ligand were more exacerbated in phenotype due to their locating on the surface of a structural element, i.e., an α helix. Together, our observations suggest a crucial role for the charge at these positions, not only for appropriate electrostatic interaction, but also for the local context of the ligand-binding pocket.

R280 of GMR-α Contributes to Ligand Recognition by a Factor of 10. The importance of electrostatic interactions in hormone–receptor recognition was previously identified for hGH. Indeed, mutations at Arg residues present on hGH were shown to affect association by a factor of 20, although each Arg individually may not have contributed by more than a factor of 2–3 to the on rate (35). In contrast, we identify here a single Arg at position 280 on GMR-α that contributes to the on rate by a factor of 10, and to the off rate by only a factor of 2, indicating its crucial role in ligand recognition. Interestingly, the nature of ligand binding for the GMR-αR280M–wild-type βc complex is intrinsically different from that established for wild-type GMR-α alone, despite the fact that the Kds for both receptors were in the same nM range. The low affinity of GMR-α binding to the ligand in the absence of βc may be attributed mainly to a major difference in the off rate when compared to that of the GMR-α–βc complex (5, 8, and our unpublished results), whereas the on rates were not significantly different,

Table 3. *Kinetic Association Constants of Wild-type and Mutant GMR-α*

GMR α + β	Antibody reactivity	Kinetic constants			Dissociation constants
	OD_{490}	K_{on}	K_{off}	K_{off}/K_{on}	Kd
	Abs.	$min^{-1}M^{-1}$	min^{-1}	*nM*	*nM*
wild type	0.241	1.3×10^8	5.6×10^{-3}	0.04	0.03
R280M	0.210	1.4×10^7	1.3×10^{-2}	0.93	3.0
D278A/V279A	0.653	5.2×10^6	5.1×10^{-3}	0.98	1.33
D278Q/V279Q	ND	7.5×10^6	8.2×10^{-3}	1.09	1.98
D278A	0.481	3.8×10^6	3.2×10^{-3}	0.84	2.5
D278N	ND	1.4×10^7	2.0×10^{-2}	1.43	0.59
I281A/L282A	ND	1.1×10^8	6.0×10^{-3}	0.06	0.05
I281Q/L282Q	0.297	3.4×10^7	8.2×10^{-3}	0.24	0.09
R258Q	0.285	0.9×10^8	6.2×10^{-3}	0.07	0.12

The kinetic association (K_{on}) and kinetic dissociation (K_{off}) constants of wild-type and mutated GMR-α were determined by using transfected NIH 3T3 cells as described in Materials and Methods and as shown in Fig. 4. The dissociation constants determined at equilibrium were estimated by analysis of full saturation curves for each mutant, using the program ALLFIT (9, 26). The reactivity of the different GMR-α mutants with the monoclonal anti–GMR-α were determined by immunoperoxidase as described in Fig. 2.

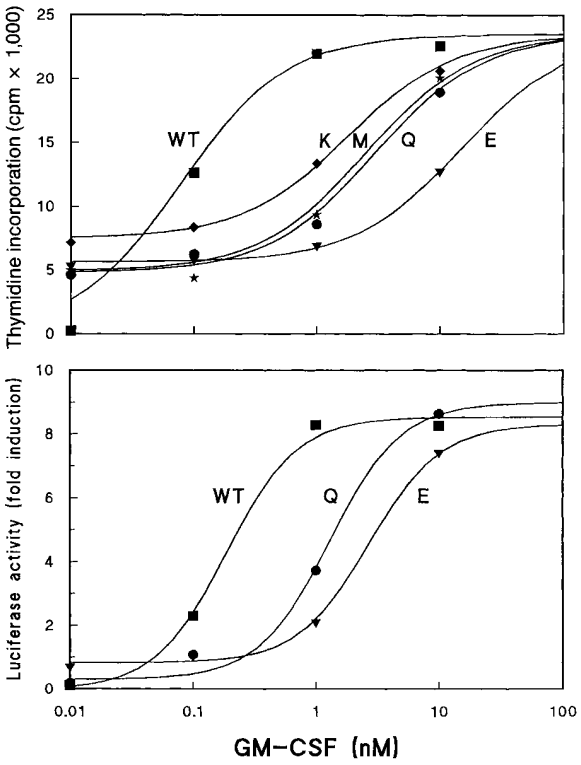

Figure 5. Ligand-induced biological response of NIH 3T3 cells expressing both GMR-αR280 mutants and βc. (*Top*) NIH 3T3 cells were co-transfected with GMR-αR280 mutants and βc. Transfected cells were then incubated for 40 h in serum-free medium supplemented with the indicated concentrations of GM-CSF. Cell proliferation was evaluated by [^{3}H]thymidine incorporation as described in Materials and Methods. Data are the mean of triplicate cultures. For each point, the standard error was no more 15% of mean values. (*Bottom*) NIH 3T3 cells were transfected with GMR-α mutants, βc, and c-fos promoter reporter construct. Transfected cells were then incubated for 24 h in serum-free medium supplemented with the indicated concentrations of GM-CSF. c-fos promoter activity was evaluated by measuring luciferase activity in cell extracts as described in Materials and Methods. Data are the mean of duplicate cultures.

suggesting that recruitment of βc into the complex results in stabilization. In contrast, mutations at position R280 of GMR-α resulted in a drastic decrease in the on rate when wild-type βc was present, indicating its crucial role in the association step. Our observations further underscore the importance of kinetic studies for molecular recognition processes.

Mutations of R280 differ from the mutations observed with Asp278 with regards to their immunoreactivities with a monoclonal antibody shown previously to prevent GM-CSF binding. Thus, all R280 mutations and wild-type GMR-α reacted with the antibody, whereas all D278 mutants displayed enhanced immunoreactivity, suggesting a structural difference and the possibility of intrachain salt bridging with a positively charged residue, Lys191, on the linker region of GMR-α. It is thus possible that the β turn which presents R280 to the ligand is held in place by two structural elements, a salt bridge conferred by Asp278 and the π-charge interactions assigned to the WSXWS box with a conserved Arg in the F′ strand, as discussed underneath (Fig. 1 and reference 36).

GMR-α and βc Preassociate in the Absence of Ligand. The fact that GMR-αR280 mutants do not bind GM-CSF when transfected alone but do so in the presence of βc, is consistent with the view that GMR-α and βc associate in

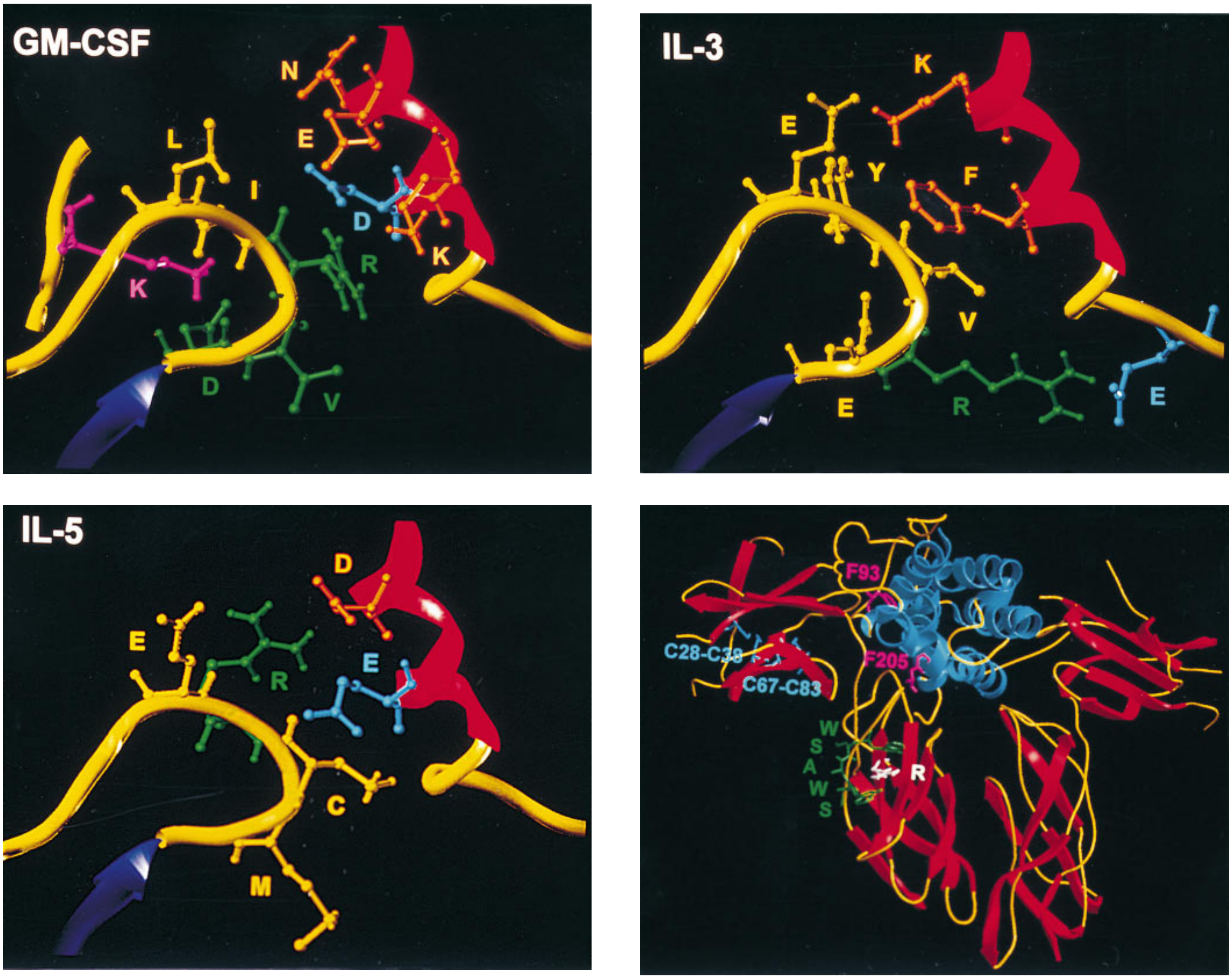

humil5r	280	D L	S K Y D V Q V R A A	V S S M C R E A G L W S E	W S Q P I Y V . N D	E H	315
humgmcsfr	266	P R	A K H S V K I R A A	***D*** . . V ***R*** I L . . N W S S	W S E A I E F G S D	D G	298
humil3r	246	N P	G T Y T V Q I R A R	E . . R V Y E . . F L S A	W S T P Q R F E C D	Q E	278
humil6r	265	S G	L R H V V Q L ***R A*** Q	E . ***E F*** G Q ***G*** . ***E*** W S E	W S P E A M G . T ***P***	W T	297
humepor	190	G R	T R Y T F A V R A R	M A . E P S ***F*** G G F W S A	W S E P V S L L T P	S D	223
fn10	1479	P G	V D Y T I T V Y A V	T . . . G ***R G D*** S P A S S	K P I S I N Y R T -	- -	1509

F/F′ G/G′

Figure 6. The F′–G′ loop of the second fibronectin domain of the GM-CSF, IL-3, and -5 α chain receptors: sequence alignment and three-dimensional models and homology modeling of the erythropoietin receptor complex with its ligand. The alignment is adapted from Bazan (14) and Goodall et al. (19). Residues in bold are shown through site-directed mutagenesis to be important for proper ligand binding (*humgmcsfr*, GMR-α, shown herein; *humil6r*, IL-6R-α (17); *fn10*, fibronectin type III tenth repeat (16); *humepor*, EpoR (41, 42). Conserved residues within the F′ and G′ strands are boxed, as well as the conserved WSXWS sequence. Comparison of the F′–G′ loop (*yellow*) facing helix D (*red*) of the ligand in the GMR-α, IL-3R-α, and IL-5R-α models, highlights a possible electrostatic interaction between a positively charged residue, Arg (*green*), and a negatively charged residue, Asp or Glu (*blue*). In GMR-α, R280 is at the tip of the β turn pointing towards the ligand, whereas the aspartic acid (D278, *green*) is in the vicinity of a lysine (K191, *magenta*) located in the linker region between the two fibronectin domains. Note that in the IL-3 model, an aromatic residue on the F′–G′ loop, Tyr261, is close to another aromatic residue, Phe113 from helix D. In the lower right panel, the extracellular domains of the two Epo receptor chains are shown complexed with the modelized Epo hormone. The Epo–EpoR_2 complex is based on the structure of the GH–GHR_2 complex, and was generated as described in the Materials and Methods. The π-charge interaction in EpoR consisting of one arginine (*white*) and two tryptophan (*green*) from the WSXWS motif is illustrated. The two disulfide bridges formed between the four conserved cysteine are shown in blue.

the absence of GM-CSF (9, 37). This preassociation is nonetheless of low affinity, and the presence of ligand results in stabilization of the α–β complex by 1,000-fold (9). Although βc does not bind GM-CSF by itself, previous data indicate that it can do so when associated with GMR-α. The contact point was identified by scanning mutagenesis of GM-CSF (31) and sequence alignment of GHR with βc (19). Consistent with this result, our data clearly indicate that βc binds the ligand even when associated with an α chain that, by itself, no longer recognizes the ligand. In addition, our observations also suggest that the association of GMR-α with βc is unlikely to generate additional GM-CSF binding sites on GMR-α beyond those affected by the R280 mutations.

Role of the F′–G′ Loop of Cytokine Receptors in Ligand Binding. Evidence is provided here that mutagenesis of members of the superfamily of cytokine receptors can be directed to specific residues that are predicted to be at the ligand–receptor interface through homology modeling with the x-ray crystal structure of the hGH bound to its receptor. It was previously shown that the functional interface of growth hormone with its receptor is much smaller than the physical interface and that electrostatic interactions are crucial for the first step in ligand–receptor recognition (35). Our data underscores the importance of a single charged residue at the F′–G′ loop of the fibronectin-like domain of the GM-CSF receptor, R280. For the GM-CSF receptor complex, data reported here for GMR-α and elsewhere for βc and GM-CSF indicate that the functional interface may be restricted to a limited number of residues, GMR-αR280, βc His367 (29, 30) and Tyr421 (38), and GM-CSF Asp112 and Glu21 (31). Furthermore, the on/off kinetics suggest that the GMR-αR280–GM-CSFD112 interaction may determine the recognition step, whereas the association with βc would stabilize the complex possibly through interaction of H367 and Tyr421 with the ligand.

Primary sequence alignment of the three closest members of the cytokine receptors superfamily, IL-3R-α, -5R-α, and GMR-α highlights the presence of one Arg at the F′–G′ loop in an otherwise diverging context (Fig. 6). Interestingly, the IL-3 and -5 receptor complex models reveal that a negatively charged residue (Glu or Asp) on the ligand is in close contact with the Arg of the F′–G′ loop, indicating a potential electrostatic interaction. Thus, the contribution of the Arg residue to ligand recognition may also be extended to these receptors. Sequence divergence in this loop among the GM-CSF, IL-3, and -5 α chain receptors suggest that this region is likely to be important for the observed specificity of the corresponding receptor subunit.

Furthermore, the F–G loop has been shown to contain binding determinants. Short peptides containing the sequence Arg-Gly-Asp (RGD) from the F–G loop of the tenth fibronectin type III repeat specifically block interactions with integrins by binding integrins (39). The F′–G′ loop of IL-6R-α contains residues that are critical for IL-6 binding: E278-F279 and G282-E283 (17). Similarly, recent data suggest the involvement of Y421 at the F′–G′ loop of βc in high-affinity GM-CSF binding (38). Moreover, the F′–G′ loop of cytokine receptors has, at its COOH-terminal end, a highly conserved WS box that plays a crucial role in maintaining the structure required for the presentation of side chains involved in ligand binding (36).

The modeling of the Epo receptor and hormone was performed using the same technique to compare our modeling approach with a cytokine receptor of known crystal structure (Fig. 6). Our model for EpoR illustrates the π-cation interaction between the two Trp of the WSXWS motif and an Arg of the F' strand that was also observed in the crystal structure (40). Furthermore, the two disulfide bridges identified between the four conserved Cys in the crystal structure are present in our model. Finally, our EpoR model shows two phenylalanines, Phe93 (E–F loop) and Phe205 (F′–G′ loop), that point towards the hormone consistent with their locating within the hydrophobic core formed between the peptide and the receptor in the crystal structure (40) as well as their importance in ligand binding (41, 42).

In summary, the presence of a highly conserved structural element in the F′–G′ loop, the WS motif, imposes a β turn to a loop that is highly divergent in sequence, allowing the conserved Arg to be oriented towards the ligand and further strengthens the possibility that this loop may be involved in ligand interaction. The presence of the integrin-binding determinant RGD in the F–G loop of the fibronectin, which does not have a WS box, further underscores the crucial role of electrostatic interactions in ligand binding for cytokine receptors with fibronectin-like domains.

This work was supported by grants from the Medical Research Council of Canada, and studentships from the Cancer Research Society Inc. (D. Rajotte) and Biron Diagnostiques (C. Cadieux). T. Hoang is a Senior Scientist from the Fonds de la Recherche en Santé du Québec, Quebec, Canada.

The authors wish to thank Drs. Peter W. Schiller, Yvan Guidon, and Rafick-Pierre Sékaly for critical comments, and Minh Dang Nguyen for his help with GMR-α mutagenesis. The expert secretarial assistance of Magali Domin is acknowledged.

Address correspondence to Dr. Trang Hoang, Clinical Research Institute of Montreal, 110 Pine Ave. West, Montréal, Québec H2W 1R7, Canada.

Received for publication 26 December 1996 and in revised form 27 March 1997.

References

1. Metcalf, D. 1993. Hematopoietic regulators: redundancy or subtlety? *Blood*. 82:3515–3523.
2. Gasson, J.C. 1991. Molecular physiology of granulocyte–macrophage colony-stimulating factor. *Blood*. 77:1131–1145.
3. Rajotte, D., P. Haddad, A. Haman, E.J. Cragoe, and T. Hoang. 1992. Role of protein kinase C and the Na^+/H^+ antiporter in suppression of apoptosis by granulocyte macrophage colony stimulating factor and interleukin-3. *J. Biol. Chem*. 267:9980–9987.
4. Caceres-Cortes, J., D. Rajotte, J. Dumouchel, P. Haddad, and T. Hoang. 1994. Product of the steel locus suppresses apoptosis in hemopoietic cells. Comparison with pathways activated by granulocyte macrophage colony-stimulating factor. *J. Biol. Chem*. 269:12084–12091.
5. Gearing, D.P., J.A. King, N.M. Gough, and N.A. Nicola. 1989. Expression cloning of a receptor for human granulocyte–macrophage colony-stimulating factor. *EMBO (Eur. Mol. Biol. Organ.) J.* 8:3667–3766.
6. Hayashida, K., T. Kitamura, D.M. Gorman, K. Arai, T. Yokota, and A. Miyajima. 1990. Molecular cloning of a second subunit of the receptor for human granulocyte–macrophage colony-stimulating factor (GM-CSF): reconstitution of a high affinity GM-CSF receptor. *Proc. Natl. Acad. Sci. USA*. 87:9655–9659.
7. Onetto-Pothier, N., N. Aumont, A. Haman, C. Bigras, G.G. Wong, S.C. Clark, A. De Léan, and T. Hoang. 1990. Characterization of granulocyte–macrophage colony-stimulating factor receptor on the blast cells of acute myeloblastic leukemia. *Blood*. 75:59–66.
8. Nicola, N.A., and D. Metcalf. 1991. Subunit promiscuity among hemopoietic growth factor receptors. *Cell*. 67:1–4.
9. Hoang, T., A. De Lean, A. Haman, V. Beauchemin, T. Kitamura, and S.C. Clark. 1993. The structure and dynamics of the granulocyte macrophage colony-stimulating factor receptor defined by the ternary complex model. *J. Biol. Chem*. 268:11881–11887.
10. Eder, M., J.D. Griffin, and T.J. Ernst. 1993. The human granulocyte–macrophage colony-stimulating factor receptor is capable of initiating signal transduction in NIH 3T3 cells. *EMBO (Eur. Mol. Biol. Organ.) J.* 12:1647–1656.
11. Sasaki, K., S. Chiba, Y. Hanazono, H. Mano, Yα. Yazaki, and H. Hirai. 1993. Coordinate expression of the α and β chains of human granulocyte–macrophage colony-stimulating factor receptor confers ligand-induced morphological transformation in mouse fibroblasts. *J. Biol. Chem*. 268:13697–13702.
12. Lia, F., D. Rajotte, S.C. Clark, and T. Hoang. 1996. A dominant negative GM-CSF receptor α chain reveals the multimeric structure of the receptor complex. *J. Biol. Chem*. 271: 28287–28293.
13. Rajotte, D., H.B. Sadowski, A. Haman, K. Gopalbhai, S. Meloche, L. Liu, G. Krystal, and T. Hoang. 1996. Contribution of both STAT and SRF/TCF to c-fos promoter activation by GM-CSF. *Blood*. 88:2906–2916.
14. Bazan, J.F. 1990. Structural design and molecular evolution of a cytokine receptor superfamily. *Proc. Natl. Acad. Sci. USA*. 87:6934–6938.
15. de Vos, A.M., M. Ultsch, and A.A. Kossiakoff. 1992. Human growth hormone and extracellular domain of its receptor: crystal structure of the complex. *Science (Wash. DC)*. 255: 306–312.
16. Leahy, D.J., I. Aukhil, and H.P. Erickson. 1996. 2.0 Å crystal structure of a four-domain segment of human fibronectin encompassing the RGD loop and synergy region. *Cell*. 84: 155–164.
17. Yawata, H., K. Yasukawa, S. Natsuka, M. Murakami, K. Yamasaki, M. Hibi, T. Taga, and T. Kishimoto. 1993. Structure–function analysis of human IL-6 receptor: dissociation of amino acid residues required for IL-6 binding and for IL-6 signal transduction through gp130. *EMBO (Eur. Mol. Biol. Organ.) J.* 12:1705–1712.
18. Quelle, F.W., N. Sato, B.A. Witthuhn, R.C. Inhorn, M. Eder, A. Miyajima, J.D. Griffin, and J.N. Ihle. 1994. JAK2 associates with the βc chain of the receptor for granulocyte–macrophage colony-stimulating factor, and its activation requires the membrane-proximal region. *Mol. Cell. Biol*. 14: 4335–4341.
19. Goodall, G.J., C.J. Bagley, M.A. Vadas, and A.F. Lopez. 1993. A model for the interaction of the GM-CSF, IL-3 and IL-5 receptors with their ligands. *Growth Factors*. 8:87–97.
20. Diederichs, K., T. Boone, and P.A. Karplus. 1991. Novel fold and putative receptor binding site of granulocyte–macrophage colony-stimulating factor. *Science (Wash. DC)*. 254: 1779–1782.
21. Rozwarski, D.A., A.M. Gronenborn, G.M. Clore, J.F. Bazan, A. Bohm, A. Wlodawer, M. Hatada, and P.A. Karplus. 1994. Structural comparisons among the short-chain helical cytokines. *Structure (Lond.)*. 2:159–173.
22. Feng, Y., B.K. Klein, and C.A. McWherter. 1996. Three-dimensional solution structure and backbone dynamics of a variant of human interleukin-3. *J. Mol. Biol*. 259:524–541.
23. Bazan, J.F. 1990. Hemopoietic receptors and helical cytokines. *Immunol. Today*. 11:350–354.
24. Hercus, T.R., B. Cambareri, M. Dottore, J. Woodcock, C.J. Bagley, M.A. Vadas, M.F. Shannon, and A.F. Lopez. 1994. Identification of residues in the first and fourth helices of human granulocyte–macrophage colony-stimulating factor involved in biologic activity and in binding to the α- and β-chains of its receptor. *Blood*. 83:3500–3508.
25. Rodriguez-Cimadevilla, J.C., V. Beauchemin, L. Villeneuve, L. Letendre, A. Shaw, and T. Hoang. 1990. Coordinate secretion of interleukin-1β and granulocyte–macrophage colony stimulating factor by the blast cells of acute myeloblastic leukemia: role of interleukin-1 as an endogenous inducer. *Blood*. 76:1481–1489.
26. DeLéan, A.P.J., P.J. Munson, and D. Rodbard. 1978. Simultaneous analysis of families of sigmoidal curves: application to bioassay, radioligand assay, and physiological dose-response curves. *Am. J. Physiol*. 235:E97–E102.
27. Wells, J.A. 1996. Binding in the growth hormone receptor complex. *Proc. Natl. Acad. Sci. USA*. 93:1–6.
28. Clackson, T., and J.A. Wells. 1995. A hot spot of binding energy in a hormone-receptor interface. *Science (Wash. DC)*. 267:383–386.
29. Woodcock, J.M., B. Zacharakis, G. Plaetinck, C.J. Bagley, S. Qiyu, T.R. Hercus, J. Tavernier, and A.F. Lopez. 1994. Three residues in the common β chain of the human GM-CSF, IL-3 and IL-5 receptors are essential for GM-CSF and IL-5 but not IL-3 high affinity binding and interact with Glu21 of GM-CSF. *EMBO (Eur. Mol. Biol. Organ.) J.* 13: 5176–5185.
30. Lock, P., D. Metcalf, and N.A. Nicola. 1994. Histidine-367 of the human common β chain of the receptor is critical for high-affinity binding of human granulocyte–macrophage col-

ony-stimulating factor. *Proc. Natl. Acad. Sci. USA*. 91:252–256.

31. Lopez, A.F., M.F. Shannon, T. Hercus, N.A. Nicola, B. Cambareri, M. Dottore, M.J. Layton, L. Eglinton, and M.A. Vadas. 1992. Residue 21 of human granulocyte–macrophage colony-stimulating factor is critical for biological activity and for high but not low affinity binding. *EMBO (Eur. Mol. Biol. Organ.) J.* 11:909–916.
32. Kaushansky, K., S.G. Shoemaker, S. Alfaro, and C. Brown. 1989. Hematopoietic activity of granulocyte–macrophage colony-stimulating factor is dependent upon two distinct regions of the molecule: functional analysis based upon the activities of interspecies hybrid growth factors. *Proc. Natl. Acad. Sci. USA*. 86:1213–1217.
33. Clark-Lewis, I., A.F. Lopez, L.B. To, M.A. Vadas, J.W. Schrader, L.E. Hood, and S.B. Kent. 1988. Structure–function studies of human granulocyte–macrophage colony-stimulating factor. Identification of residues required for activity. *J. Immunol.* 141:881–889.
34. Park, L.S., D. Friend, S. Gillis, and D.L. Urdal. 1986. Characterization of the cell surface receptor for granulocyte–macrophage colony-stimulating factor. *J. Biol. Chem.* 261:4177–4183.
35. Cunningham, B.C., and J.A. Wells. 1993. Comparison of a structural and a functional epitope. *J. Mol. Biol.* 234:554–563.
36. Baumgartner, J.W., C.A. Wells, C.M. Chen, and M.J. Waters. 1994. The role of the WSXWS equivalent motif in growth hormone receptor function. *J. Biol. Chem.* 269:29094–29101.
37. Ronco, L.V., S.L. Silverman, S.G. Wong, D.J. Slamon, L.S. Park, and J.C. Gasson. 1994. Identification of conserved amino acids in the human granulocyte–macrophage colony-stimulating factor receptor α subunit critical for function. Evidence for formation of a heterodimeric receptor complex prior to ligand binding. *J. Biol. Chem.* 269:277–283.
38. Woodcock, J.M., C.L. Bagley, B. Zacharakis, and A.F. Lopez. 1996. A single tyrosine residue in the membrane proximal domain of the GM-CSF, IL-3 and IL-5 receptor common β chain is necessary and sufficient for high affinity binding and signalling by all three ligands. *J. Biol. Chem.* 271: 25999–26006.
39. Ruoslahti, E. 1996. Integrin signaling and matrix assembly. *Tumor Biol.* 17:117–124.
40. Livnah, O., E.A. Stura, D.L. Johnson, S.A. Middleton, L.S. Mulcahy, N.C. Wrighton, W.J. Dower, L.K. Jolliffe, and I.A. Wilson. 1996. Functional mimicry of a protein hormone by a peptide agonist: the EPO receptor complex at 2.8 Å. *Science (Wash. DC).* 273:464–471.
41. Middleton, S.A., D.L. Johnson, R. Jin, F.J. Mahon, A. Collins, J. Tullai, R.H. Gruninger, L.K. Jolliffe, and L.S. Mulcahy. 1996. Identification of a critical ligand binding determinant of the human erythropoietin receptor: evidence for common ligand binding motifs in the cytokine receptor family. *J. Biol. Chem.* 271:14045–14054.
42. Middleton, S.A., D.L. Johnson, F.X. Farrell, F.J. McMahon, R.H. Gruninger, J. Tullai, F.P. Barbone, O. Livnah, L.S. Mulcahy, I.A. Wilson, and L.K. Jolliffe. 1996. Critical erythropoietin (Epo) binding determinants on the Epo receptor also interact with an Epo mimetic peptide. *Blood*. 88 (Suppl.) 1:661a. (Abstr.)